Boston University

OpenBU **http://open.bu.edu**

Boston University Theses & Dissertations Boston University Theses & Dissertations

2018

The role of glutaredoxin-1 on B16F0 melanoma growth and angiogenesis in diet-induced diabetic mice

https://hdl.handle.net/2144/31165

Downloaded from DSpace Repository, DSpace Institution's institutional repository

BOSTON UNIVERSITY

SCHOOL OF MEDICINE

Thesis

THE ROLE OF GLUTAREDOXIN-1 ON B16F0 MELANOMA GROWTH AND ANGIOGENESIS IN DIET-INDUCED DIABETIC MICE

by

BRIAN SUNG HO CHONG

B.S., University of Washington, 2015

Submitted in partial fulfillment of the

requirements for the degree of

Master of Science

2018

© 2018 by
BRIAN SUNG HO CHONG
All rights reserved

Approved by

First Reader _____

Reiko Matsui, M.D.
Assistant Professor of Medicine

Second Reader _____

Markus Bachschmid, Ph.D.
Assistant Professor of Medicine

ACKNOWLEDGMENTS

I would like to express my deepest gratitude towards my primary investigator, Dr. Reiko Matsui, who made this study possible through her wisdom and thorough guidance.

I would also like to specially thank Dr. Markus Bachschmid, Dr. Yoshimitsu Yura, Dr. Beatriz Ferrán Pérez, Dr. Yuko Tsukahara, Dr. Francesca Seta, Dr. Jingyan Han, and the Vascular Biology Unit of the Whitaker Cardiovascular Institute for their supervision, guidance, and support in the completion of this study.

THE ROLE OF GLUTAREDOXIN-1 ON B16F0 MELANOMA GROWTH AND ANGIOGENESIS IN DIET-INDUCED DIABETIC MICE

BRIAN SUNG HO CHONG

ABSTRACT

Objectives: Recent studies have elucidated that diabetes mellitus (DM) patients exhibit an accelerated tumor progression, but the mechanism of its regulation is not yet fully understood. The following study seeks to examine the role of angiogenic factors in the growth of subcutaneously injected melanoma cancer using a diet-induced type II diabetic mouse model.

Methods: C57BL/6 mice were fed either a regular or high-fat, high-sucrose (HFHS) diet for 2 months (T2DM model; confirmed through a GTT) and subcutaneously injected with B16F0 melanoma cells. After a 1-week or 2-week incubation period, the tumor was extracted to examine its size, weight, vascularity, and gene/protein expression. *In vitro* studies were performed using endothelial cells to assess the effects of high-glucose on endothelial cell proliferation, migration, and tube formation. GLRX expression was examined in both tumor samples and endothelial cells.

Results: The results of the study showed that T2DM induced by a HFHS diet is able to promote tumor growth in both weight (2-week, $p = 0.0070$) and volume (1-week, $p = 0.0351$; 2-week, $p = 0.0002$). Tumors extracted from the HFHS diet group showed reduced expressions of angiogenic markers (ACTA2 (1-week, $p = 0.0239$; 2-week, $p = 0.0123$), KDR (1-week, $p = 0.0091$)) by western blot and a slightly reduced trend of angiogenesis (PECAM1) in histological analyses. GLRX expression was reduced in

HFHS tumor samples (1-week, $p = 0.0090$) and, interestingly, lower amounts of GSH adducts (2-week, $p = 0.0317$) could be seen in 2-week tumors as well. *In vitro* studies of endothelial cells showed reduced trends of endothelial cell function (proliferation, migration, and tube formation) in high glucose medium. Also, it has been observed that high glucose may be able to stimulate GLRX expression in endothelial cells.

Conclusion: The results of the following study have confirmed that B16F0 melanoma growth is, in fact, augmented in diet-induced diabetic mice; however, the vascularity and levels of angiogenic markers from the tumor tissues did not parallel the growth in its size. *In vitro* studies suggested that high glucose can impair EC function (i.e. proliferation, migration, and tube formation capabilities) as well as promote GLRX expression, which may be related to this discrepancy. Glutaredoxin-1 (GLRX), an enzyme which controls redox signaling, is upregulated in DM. Endothelial cell-specific GLRX overexpression in transgenic mice was found to stimulate subcutaneously injected melanoma (B16F0) growth, despite hindering limb revascularization after hind limb ischemia. The augmented tumor progression in DM may be associated with GLRX upregulation, alongside impaired ischemic limb revascularization and tumor angiogenesis; however, the mechanism of tumor growth in diabetes still lies inconclusive and further studies need to be examined to elucidate this phenomenon.

TABLE OF CONTENTS

LIST OF TABLES

LIST OF FIGURES

LIST OF ABBREVIATIONS

ACTA2 ..... Actin, Alpha 2, Smooth Muscle, Aorta

ACTB ..... Actin Beta

ANGPT2 ..... Angiopoetin 2

BU ..... Boston University

CD ..... Control Diet

cDNA ..... Complementary Deoxyribonucleic Acid

CLI ..... Critical Limb Ischemia

DM ..... Diabetes Mellitus

EC ..... Endothelial Cell

FLT1 ..... Fms Related Tyrosine Kinase 1

GLRX ..... Glutaredoxin 1

GSH ..... Glutathione

GTT ..... Glucose Tolerance Test

HDMVEC ..... Human Dermal Microvascular Endothelial Cell

HFHS ..... High-Fat, High-Sucrose

HIF1A ..... Hypoxia Inducible Factor 1 Alpha Subunit

KDR ..... Kinase Insert Domain Receptor

MMP2 ..... Matrix Metallopeptidase 2

mRNA ..... Messenger Ribonucleic Acid

NC ..... Normal Chow

NF-κB ..... Nuclear Factor Kappa-B

NPDR ..... Non-Proliferative Diabetic Retinopathy

PAD ..... Peripheral Artery Disease

PDR ..... Proliferative Diabetic Retinopathy

PECAM1 ..... Platelet and Endothelial Cell Adhesion Molecule 1

PTP1B ..... Protein Tyrosine Phosphatase 1B

RAC1 ..... Rac Family Small GTPase 1

RNS ..... Reactive Nitrogen Species

ROS ..... Reactive Oxygen Species

RT-qPCR ..... Quantitative Real-Time Polymerase Chain Reaction

SERCA2 ..... Sacroplasmic-Endoplasmic Reticulum Calcium ATPase 2B

TG ..... Transgenic

TR ..... Texas Red

TXN ..... Thioredoxin

T2DM ..... Type II Diabetes Mellitus

VEGFA ..... Vascular Endothelial Growth Factor A

VM ..... Vasculogenic Mimicry

WNT5A ..... WNT Family Member 5A

WT ..... Wild Type

INTRODUCTION

Diabetes mellitus (DM) is a chronic metabolic disorder that displays a broad spectrum of clinical manifestations in a variety of different organ systems. Of these, DM has been shown to exhibit higher rates of mortality with cancer (Barone et al., 2008) and augment the progression of certain types of neoplasms (Barone et al., 2010; Giovannucci et al., 2010; Nunez et al., 2006). Despite an indicated linkage between DM and augmented tumor progression, the pathogenesis of such nature is still obscure. The following study seeks to explore the role of angiogenic factors in the growth of subcutaneously injected melanoma cancer using a diet-induced type II diabetic mouse model.

Type II Diabetes Mellitus (T2DM).

Diabetes mellitus (DM) is a metabolic disorder of various etiologies ranging from genetic to environmental factors. Clinically, diabetes is typically divided into two major types. Type I diabetes mellitus, previously referred to as juvenile-onset diabetes or insulin-dependent diabetes mellitus, is characterized by the body's inability to produce insulin via the destruction of insulin-producing β-cells of the pancreas, most probably through viral or immunological mechanisms (American Diabetes Association, 2010). In contrast, type II diabetes mellitus (T2DM) was previously referred to as adult-onset diabetes or non-insulin-dependent diabetes mellitus and accounts for most of the diagnosed cases of diabetes (Centers for Disease Control and Prevention, 2017). T2DM

usually develops with insulin resistance and is postulated to be a result of both genetic and lifestyle factors (American Diabetes Association, 2010).

Accounting for approximately 90 to 95 % of all diagnosed cases of diabetes, T2DM has steadily increased in the number of its diagnosis and prevalence to become one of the most prevalent diseases in the modern-day society (Centers for Disease Control and Prevention, 2017). Among various complications which diabetes causes, this study aims to elucidate the relationship between the vascular complications and the augmented tumor progression exhibited in diabetes (Cheng & Ma, 2015; Giovannucci et al., 2010; Nunez et al., 2006).

Vascular Complications of Diabetes.

DM is classically associated with two paradoxical complications in angiogenesis. There can either be a deficiency in the vascularization of peripheral tissues, which can lead to peripheral artery diseases (PAD) and critical limb ischemia (CLI), or an uncontrolled formation of premature blood vessels, such as in proliferative diabetic retinopathy (PDR) (Cheng & Ma, 2015).

Critical limb ischemia is considered to be the end stage of PAD. PAD is typically initiated by obstructive atherosclerotic diseases; and poor arteriogenesis and angiogenesis potential (e.g. observed in diabetes) can cause severe necrotic cases, i.e. critical limb ischemia (Varu, Hogg, & Kibbe, 2010). In fact, it has been reported that 40 % of diabetic patients with CLI, compared with 9 % of nondiabetic patients, show a progression to gangrene and also have lower limb salvage rates compared to the latter (Varu et al.,

2010), as diabetic patients with CLI showed a significantly higher risk, 5-years follow-up, in major amputation rates with 34.1 % vs. 20.4 % (Spreen et al., 2016).

Previously, through an unpublished data, Dr. Colin Murdoch, Ph.D. (Vascular Biology Unit, BU School of Medicine) has shown that diet-induced diabetic mice exhibited significantly impaired revascularization (i.e. arteriogenesis and angiogenesis) after a hind limb ischemia procedure (**Figure 1**).

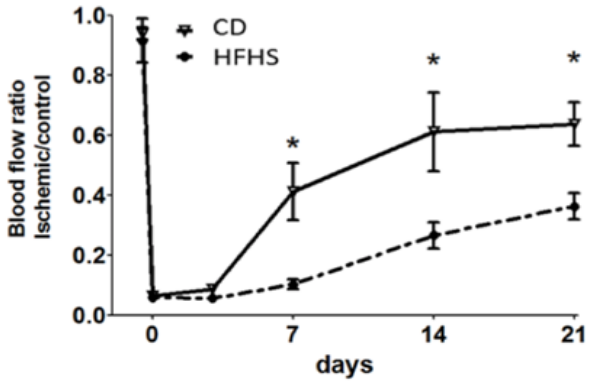

Figure 1: Blood Flow Recovery (CD vs. HFHS). The blood flow recovery of diet-induced diabetic (T2DM) mice was significantly impaired compared to the control (CD; normal chow) mice group. Blood flow ratio (*y*) was calculated using Doppler imaging of the ischemic limb / control. Ischemic hind limbs were generated on the left hind limb of the mouse through a femoral artery ligation procedure and compared to the control (right; non-ischemic) limb. Days (*x*) indicates the number of days, post-surgery. (* = $p \leq 0.05$).

The results of the data suggest that T2DM, alone, can sufficiently inhibit arteriogenesis (collateral formation) and angiogenesis (capillary formation), *in vivo*.

Diabetic retinopathy is a medical condition in which damage occurs to the small blood vessels and neurons of the retina. The disease is classified into two types: non-proliferative diabetic retinopathy (NPDR) and proliferative diabetic retinopathy (PDR).

NPDR is the early stage of the disease and symptoms include weakness in the blood vessels in the retina and microaneurysms (Duh, Sun, & Stitt, 2017). PDR is a progression of NPDR and, in contrast to the avascularity observed with NPDR, shows a rapid hypervascularity in fragile blood vessels through the expression of proangiogenic growth factors due to the hypoxic environment caused by circulation problems in the retina (Duh et al., 2017). In addition to being a pathological characteristic of microvascular complications in diabetes, persistent, uncontrolled angiogenesis is also a hallmark of cancer (Cheng & Ma, 2015; Krukovets, Legerski, Sul, & Stenina-Adognravi, 2015; Nishida, Yano, Nishida, Kamura, & Kojiro, 2006).

The Role of Angiogenesis in Tumor Growth.

Multiple factors can contribute to tumor growth. However, tumor growth is classically thought to be inseparable with angiogenesis and neovascularization (Nishida et al., 2006; Ronca, Benkheil, Mitola, Struyf, & Liekens, 2017). That is, tumor growth, as is with any other tissue, should be angiogenesis-dependent, due to the high demand for nutrition from the rapidly proliferating cells. It is interesting to note that certain tumor cells, melanoma of the several, are also known to exhibit a phenomenon known as vasculogenic mimicry when they are unable to obtain sufficient nutrients from regular angiogenesis (Delgado-Bellido, Serrano-Saenz, Fernandez-Cortes, & Oliver, 2017; Qiao et al., 2015; Ronca et al., 2017). Vasculogenic mimicry is the *de novo* formation of vessel like structures without endothelial cells. These tumor cells are able to newly form and

line blood-carrying channels, effectively mimicking a true vascular endothelium (Delgado-Bellido et al., 2017; Qiao et al., 2015; Racordon et al., 2017).

Tumor Progression in Diabetes.

As stated above, certain types of neoplasms (i.e. liver, pancreas, endometrium, colon and rectum, breast, and bladder) have been shown to exhibit a more aggressive progression with T2DM (Giovannucci et al., 2010).

Diabetes is a multifaceted metabolic syndrome as is the contributing factors that lead to tumor progression (Giovannucci et al., 2010; Vigneri, Frasca, Sciacca, Pandini, & Vigneri, 2009). Studies have tried to explain the enhanced tumor progression in diabetes with a plethora of different pathways from inflammation to insulin resistance (Chen et al., 2014; Mori et al., 2006; Novosyadlyy et al., 2010; Nunez et al., 2006); however, the effects of angiogenesis on tumor growth in T2DM is not well explored.

Glutaredoxin-1 Inhibits Endothelial Cell Migration.

Glutaredoxins are a class of redox enzymes that serve a vital role in cell signaling transduction pathways (Matsui, Watanabe, & Murdoch, 2017). Glutaredoxin-1 is a cytosolic enzyme that reduces post-translational modifications of GSH adducts in a GSH-dependent manner. Reactive oxygen species (ROS) or reactive nitrogen species (RNS) induce thiolate anions to undergo *S*-hydroxylation or *S*-nitrosylation to produce sulfenic acid and *S*-nitrosothiol, respectively. These intermediate molecules are relatively

unstable, and are stabilized by reacting with glutathiones that are abundant in the cell, through a process called *S*-glutathionylation to produce glutathione adducts. GLRX reduces these GSH adducts back into reactive thiols (Matsui et al., 2017) (**Figure 2**).

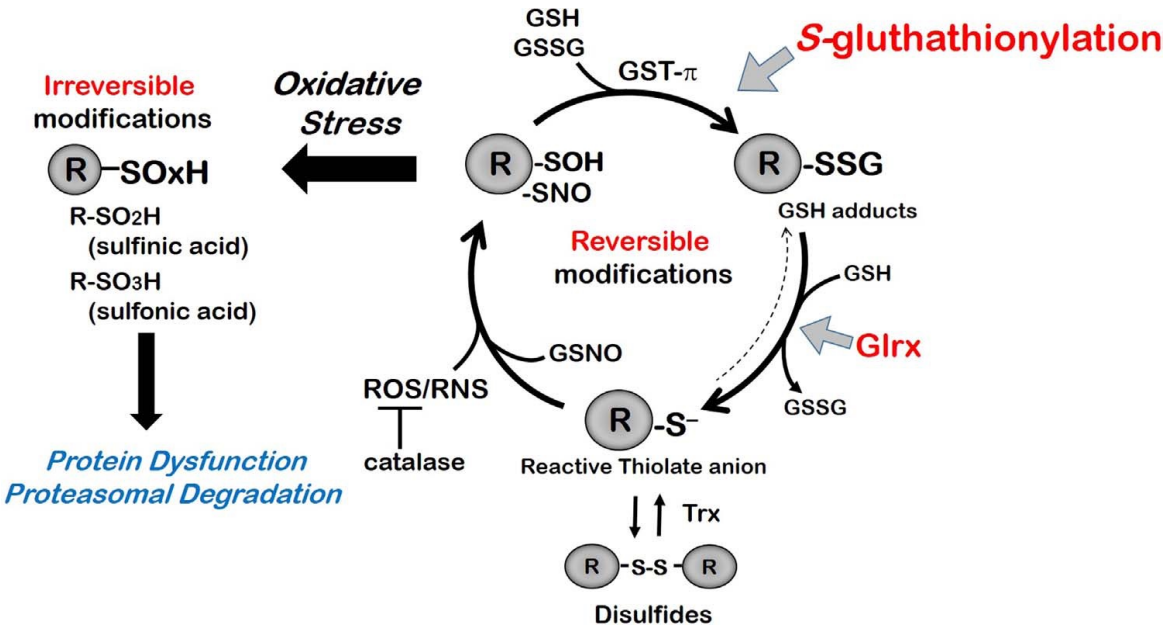

Figure 2: Glutaredoxin-1. Schematic diagram showing the role of glutaredoxin in the reversible modification of GSH adducts (Matsui et al., 2017).

Several studies have elucidated that GLRX inhibits endothelial cell migration through multiple targets within angiogenic pathways (Cohen et al., 2016; Matsui et al., 2017; Murdoch et al., 2014; Watanabe et al., 2016). In short, GLRX has been shown to take part in pathways regarding nuclear factor kappa-B (NF-κB) transcription, hypoxia inducible factor 1 α (HIF1A) stabilization, protein tyrosine phosphatase 1B (PTP1B) activation, sarcoplasmic-endoplasmic reticulum calcium ATPase 2B (SERCA2)

inhibition, and Rac family small GTPase 1 (RAC1) activation by removing GSH adducts, leading to the inhibition of endothelial cell migration (Matsui et al., 2017) (**Figure 3**).

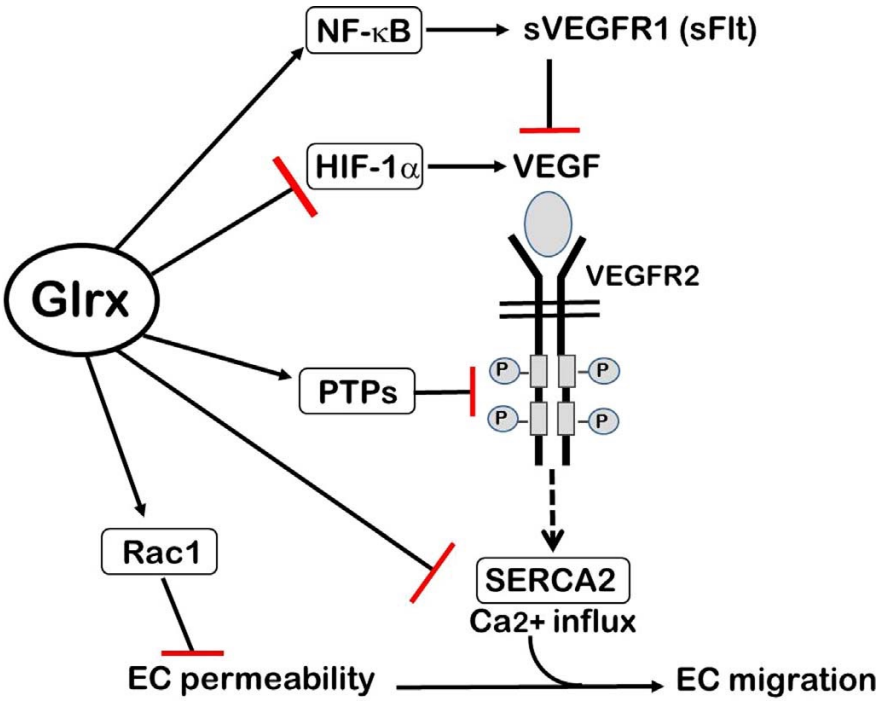

Figure 3: Glutaredoxin-1 Inhibits Endothelial Cell Migration. Schematic diagram showing the various pathways that lead to attenuated EC migration (Matsui et al., 2017).

It is shown that GLRX is upregulated in diabetic rat tissue, and high glucose increases GLRX expression (Shelton, Kern, & Mieyal, 2007). GLRX is an NF-κB dependent gene (Aesif et al., 2011) and may be induced in expression by the inflammation associated with DM. Therefore, up-regulation of GLRX may contribute to the poor angiogenesis in DM and may influence tumor growth.

SPECIFIC AIMS

Type II diabetes mellitus and cancer are two of the most common type of illnesses that can significantly burden the quality of life in the modern-day society (Giovannucci et al., 2010). Although studies have indicated a linkage between type II diabetes mellitus and augmented tumor progression, the pathogenesis of such nature is still obscure (Vigneri et al., 2009). There are studies showing enhanced tumor growth in diabetic mice, but most of these studies examine the growth and metastasis of tumor cells using a type I diabetic mouse model. The vast majority of these studies do not focus on melanoma cells and a few examine tumor angiogenesis.

The following study aims to take a first look at subcutaneous B16F0 melanoma implant growth in diet-induced type II diabetic mice with the analysis of tumor vascularity and angiogenic factors.

METHODS

Animal Model

8-weeks old, male C57BL/6 mice were either fed with a normal chow (NC) or a high-fat, high-sucrose (HFHS) diet for 2 or 3 months to generate control and T2DM models, respectively. The diabetic statuses of the mice were confirmed through a glucose tolerance test (**Figure 4**). Mice were intraperitoneally injected with D-glucose (1 mg/g of body weight) and monitored at specific time points for their blood glucose levels (Ayala et al., 2010).

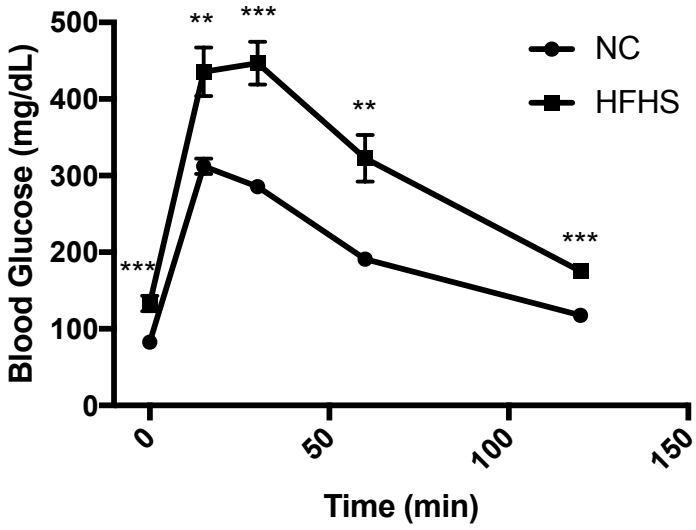

Figure 4: Glucose Tolerance Test (NC vs. HFHS). Glucose tolerance test of NC and HFHS mice. HFHS mice have a slower rate of glucose clearance, verifying diabetic status. (** = $p \leq 0.01$, *** = $p \leq 0.001$).

Mouse models were generated in 4 separate cohorts. The preliminary, or pilot, cohort was created with $n = 5$ for each group and fed with special diet for 2 months. After feasibility studies were performed, 3 more cohorts were made with a 3-month diet. Cohorts 2 and 3 had their tumor extracted 2-weeks post-injection. Cohort 4 had their tumor extracted 1-week post-injection.

B16F0 Melanoma Implants

B16F0 melanoma cells, obtained from Dr. Nader Rahimi, Ph.D. (BU School of Medicine), were cultured using Dulbecco's Modified Eagle Medium (DMEM) (Gibco) with D-Glucose (4.5 g/L), L-Glutamine, and 10 % FBS. Cells were counted using a hemocytometer after being trypsinized using 0.25 % Trypsin-EDTA (Gibco) and suspended in Growth Factor Reduced Matrigel Basement Membrane Matrix (Corning). Syringes were prepared for injection with cells at a concentration of $4 \cdot 10^5$ cells / 200 µL of Matrigel per injection.

All injections were performed in the dedicated animal surgery room of the laboratory. The mice were anesthetized using ketamine and xylazine administered through an intraperitoneal injection for a final dose of 75 mg/kg and 8.5 mg/kg, respectively. Tumor implants were administered subcutaneously on the left caudal quadrant of the dorsum of the animal. The mice were monitored until they regained consciousness and returned to the BU animal facility for the remainder of the study.

Depending on their cohort, mice were brought back 1 or 2-weeks post-injection for sample collection. The mice were anesthetized using an IP-ketamine and xylazine

injection. From each mouse, the heart, lung, liver, skeletal muscle (gastrocnemius), and 500 μL of serum were collected alongside tumor samples for future studies.

Mice were weighed before and after implantation and tumor samples were weighed and measured for their size using a digital caliper before being divided into 3 pieces for frozen and paraffin sections and biochemical analyses.

Extracted tumor samples were calculated for their volume using the ellipsoid volume formula, $V = \pi/6 \cdot L \cdot W \cdot H$ (Tomayko & Reynolds, 1989).

Human Dermal Microvascular Endothelial Cells

HDMVECn (ATCC) were cultured using EBM-2 (Lonza) basal medium with added EGM-2 MV SingleQuots (Lonza) kit, unless specified otherwise. The cells were supplied with fresh medium every 2 days and were passaged at approximately 80% confluence using 0.05 % Trypsin-EDTA (Gibco).

Western Blot

Frozen tumor samples were pulverized in liquid nitrogen using a mortar and pestle to increase the homogeneity of the sample. Protein was extracted from 50 mg of tissue samples by centrifuging (4 °C; 30’; 13400 rpm) after homogenizing the samples in lysis buffer using a MagNA Lyser (Roche) instrument.

Cellular proteins were extracted through centrifugation (4 °C; 30'; 13400 rpm) after the cells were scratched with lysis buffer using a cell scraper. Aspirated cell plates were frozen in liquid nitrogen prior to being scratched.

Protein concentration was determined using the DC Protein Assay (Bio Rad). 20 µg of protein were run on NuPAGE 4 – 12 % Bis-Tris Gels (Invitrogen) and transferred onto TransBlot Turbo Mini-size PVDF Membranes (Bio Rad) using a Trans-Blot Turbo (Bio Rad) transfer system. Membranes were washed using PBS with Tween 20 (0.1 %) (PBS-T). After blocking with PBS-T containing 3% skim milk, primary antibody reactions were carried out in PBS-T with BSA (3 %). Secondary antibody reactions were done in PBS-T with skim milk (3 %). Membranes were developed using enhanced chemiluminescence with a digital KwikQuant (Kindle Biosciences) imager and quantified using ImageJ software (NIH).

Immunohistochemistry

Immunohistochemistry analyses were performed using frozen and paraffin sections. Excised tumor samples for paraffin sections were fixed in 10 % formaldehyde overnight and transferred to PBS. Samples were embedded in paraffin and sectioned by the BU School of Medicine Immunohistochemistry Service Center.

Frozen sections were prepared by sequentially placing the tumor samples in PBS with 10 % sucrose, 20 % sucrose, and an even mixture of 20 % sucrose PBS with Tissue Plus Optimal Cutting Temperature (OCT) Compound (Fisher) embedding medium. Prepared samples were embedded in pure OCT Compound (Fisher) and sectioned using a

Leica CM1950 (Leica) cryostat. Sectioned samples were fixed using cold acetone and washed using PBS. The samples were blocked using a blocking solution (PBS-T with 3 % BSA) and incubated with a diluted primary antibody overnight at 4 °C. Both primary and secondary antibodies were diluted in the blocking solution. Alexa Fluor 594-conjugated secondary antibodies were applied at room temperature with Hoechst and incubated for 2 hours. Images were acquired using a Nikon deconvolution wide-field epifluorescence system (Nikon) in the BU core facility and analyzed using ImageJ software (NIH).

RT-qPCR

Frozen tumor samples were pulverized in liquid nitrogen using a mortar and pestle to increase the homogeneity of the sample. mRNA was extracted from 50 mg of tissue samples using a Direct-zol RNA MiniPrep Plus (Zymo Research) kit. cDNA was synthesized from either 1 µg or 500 ng of mRNA using a iScript cDNA Synthesis Kit (Bio Rad). RT-qPCR was run using a CFX96 Touch Real-Time PCR Detection System (Bio Rad).

Wound-healing Assay

HDMVEC were cultured in 0.5 % gelatin-coated plates until 80% confluence and made quiescent overnight using low-serum medium (EBM-2 basal medium with 0.1 % FBS), containing either low (1.0 g/L) or high (4.5 g/L) -glucose, without additional

growth-factors or cytokines. Scratch wounds were applied to endothelial cell monolayers using a sterile P-1000 pipette tip. Once scratched, cells were once again supplied with their respective low or high-glucose mediums with added vascular endothelial growth factor (VEGF; 50 ng/mL) (Murdoch et al., 2014). Images were taken at fixed locations along the wound at 0, 6, and 18 h using an Eclipse TS100 (Nikon) microscope with a SPOT Insight 2 MP CCD Color Digital Camera System (Spot Imaging). The images were analyzed with ImageJ software (NIH) by averaging the distances of 5 measurements per condition; this was considered as $n = 1$.

Cell Proliferation Assay

Cell proliferation assays were performed using 96 well plates (Falcon). HDMVEC were seeded at a density of $1.8 \cdot 10^3$ cells / 45 µL / well. Once the cells were attached overnight, the cells were washed with PBS and had their medium changed to low (1.0 g/L) or high (4.5 g/L)-glucose medium. The cells were incubated for 4 days and their proliferation was measured using Hoechst staining, measured with an Infinite M1000 Pro (Tecan) multifunctional monochromator based microplate reader.

Tube Formation Assay

96 well plates (Falcon) were coated with 40 µL of Growth Factor Reduced Matrigel Basement Membrane Matrix (Corning), and incubated at 37 °C for 1 hour. HDMVECn were seeded above the Matrigel matrix at a concentration of $1 \cdot 10^4$ cells / 45

μL of low (1.0 g/L) or high (4.5 g/L)-glucose medium per well. Photos of the cells were taken from 0 to 6 hours using an Eclipse TS100 (Nikon) microscope with a SPOT Insight 2 MP CCD Color Digital Camera System (Spot Imaging) using a 40X view-field. Tube formation was quantified by using Angiogenesis Analyzer for ImageJ (NIH). In short, the images were skeletonized and analyzed for the number of nodes, junctions, meshes, segments, and branches; the lengths of the segments, branches, and the total length (sum of length of segments, isolated elements, and branches); and for the total area of the meshes.

Hind Limb Ischemia

Hind limb ischemia surgeries and data were previously performed and collected by Dr. Colin Murdoch, Ph.D. (Vascular Biology Unit, BU School of Medicine). Briefly, ischemic limb revascularization was examined in NC and HFHS mice via a femoral artery ligation procedure followed by Doppler imaging (Murdoch et al., 2014).

Statistical Analysis

All group data are expressed as means ± SEM. Statistical analysis comparing two groups were carried out using a parametric, unpaired *t*-test. $p < 0.05$ was used to determine significance. All analyses were carried out using GraphPad Prism 7 and Microsoft Excel.

RESULTS

B16F0 Melanoma Growth is Significantly Promoted in Diabetic Mice.

Tumor masses excised from the HFHS group started to show an inclined tendency of growth from 1-week of incubation. The HFHS group had a slightly higher tumor weight (132.4 ± 15.23 mg, $n = 4$) compared to the NC group (98.45 ± 15.23 mg, $n = 4$) in 1 week (**Figure 5A**, $p = 0.1168$). The volume of the tumor, estimated by the ellipsoid formula (Tomayko & Reynolds, 1989), was significantly different ($p = 0.0351$) between the two groups (NC vs. HFHS; 36.37 ± 7.219 mm^3 vs. 101 ± 22.73 mm^3, $n = 4$) (**Figure 5B**). After 2 weeks of incubation (Cohorts 2 and 3), both the tumor weight (**Figure 5C**; $p = 0.007$) and volume (**Figure 5D**; $p = 0.002$) exhibited a significant difference between the two groups. The HFHS group had a larger tumor weight (1150 ± 147.6 mg, $n = 7$) and volume (1348 ± 161 mm^3, $n = 7$) compared to the NC group, whose weight and volume were 678.5 ± 43.54 mg ($n = 8$) and 514.4 ± 59.02 mm^3 ($n = 8$), respectively. The data of the tumor measurements suggest that the tumor size is significantly differentiated between the two groups within 1 to 2 weeks (**Figures 5E, 5F**).

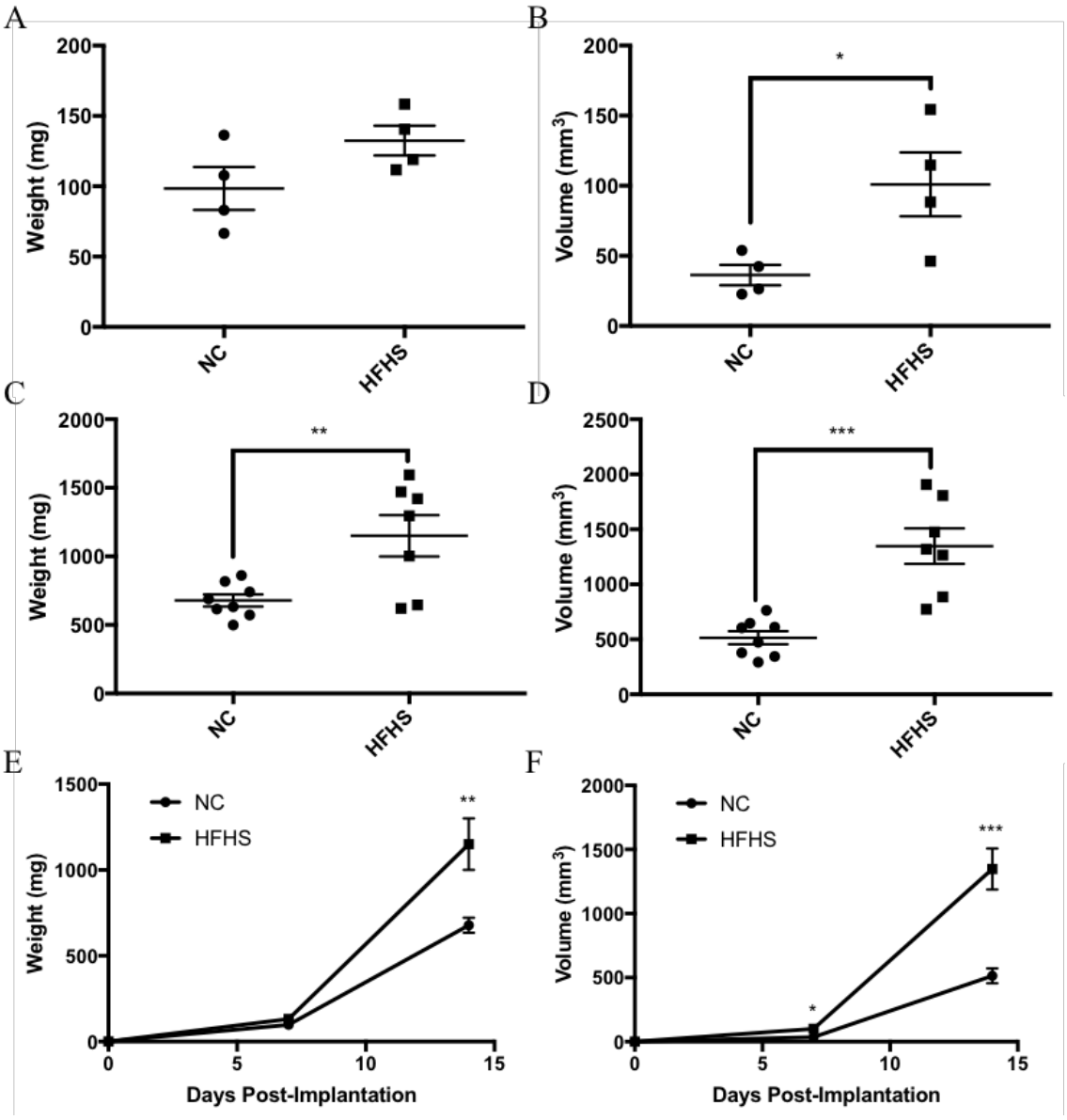

Figure 5: Tumor Weight and Volume (NC vs. HFHS). (A) 1-week tumor weight of NC vs. HFHS mice ($n = 4$, each). (B) 1-week tumor volume of NC vs. HFHS mice ($n = 4$, each). (C) 2-week tumor weight of NC vs. HFHS mice ($n = 8$ NC, $n = 7$ HFHS). (D) 2-week tumor volume of NC vs. HFHS mice ($n = 8$ NC, $n = 7$ HFHS). (E) Tumor weight vs. incubation time (NC vs. HFHS). (F) Tumor volume vs. incubation time (NC vs. HFHS). (* = $p \leq 0.05$, ** = $p \leq 0.01$, *** = $p \leq 0.001$). See appendix for individual tumor size and weight data.

Vascular Density Assessed by PECAM1 was Not Significantly Different in the Melanoma Tumors from Both Diet Groups.

Upon excision of the tumor samples, vessel structures could be observed invading into the tumor masses from the host (**Figure 6A**), supplementing the notion that tumors are capable of initiating angiogenesis for growth (Nishida et al., 2006).

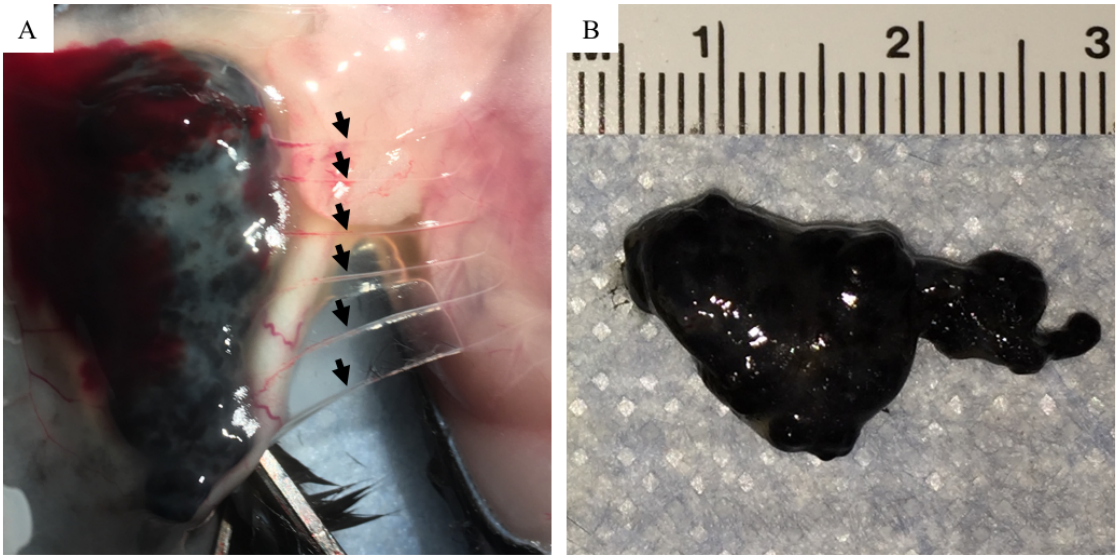

Figure 6: Tumor Mass. (A) Image of vessel structures from the host invading into the tumor mass. (B) Representative image of extracted tumor sample.

Immunohistochemistry analyses were performed using immunofluorescent PECAM1 staining to quantify the vasculature density between the two groups. Tumor sections were photographed by stitching 9 view-fields of 100 X magnifications to create one large image (**Figure 7**). The sections were analyzed using ImageJ software (NIH) by normalizing the average the density of staining within 5 random areas per sample to the

area. The results showed that there was a slightly lower density of PECAM1 staining in the 2-week tumor samples (Cohort 2) of the HFHS group (1.342 ± 0.09972 %, $n = 5$) compared to the NC group (1.635 ± 0.1418 %, $n = 5$) (**Figure 8**); however, the results were not significant ($p = 0.1291$).

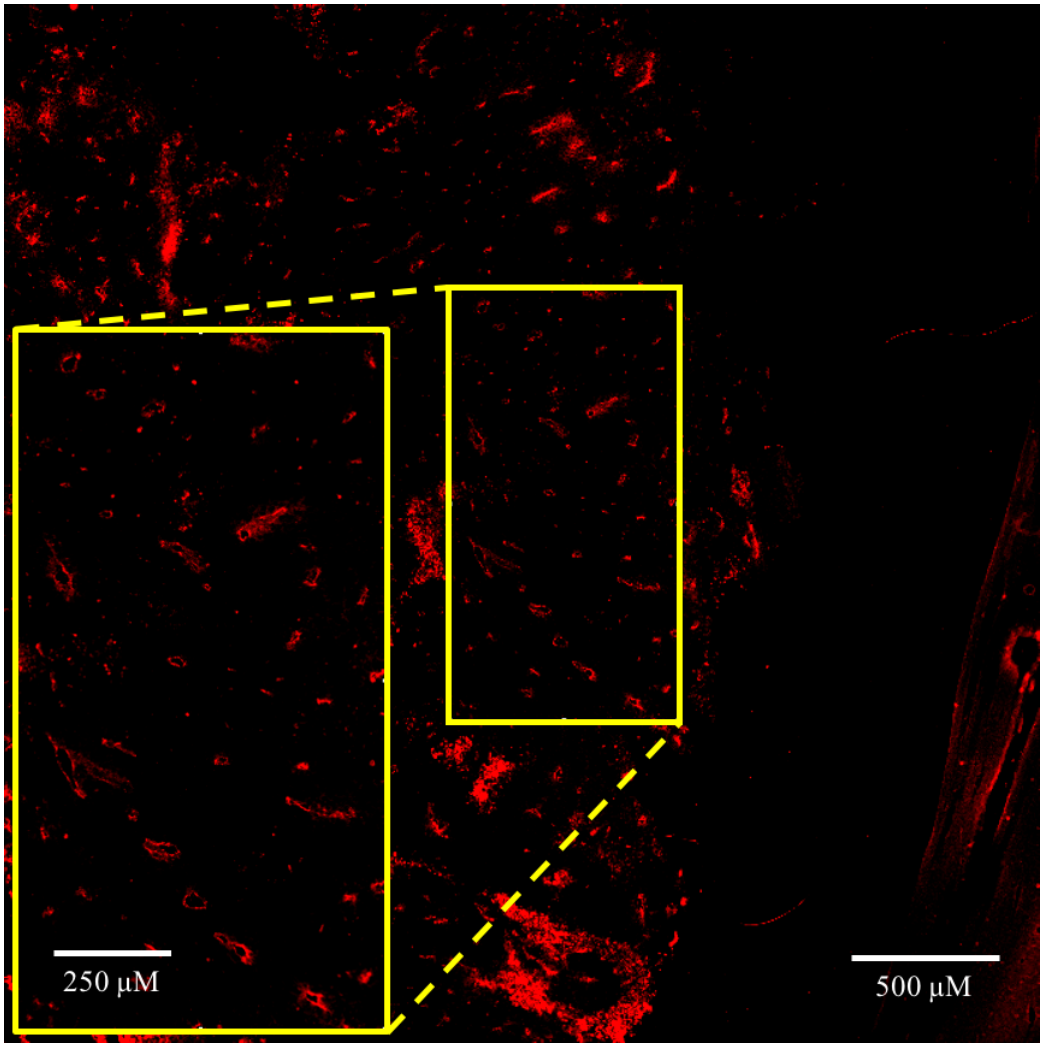

Figure 7: Immunofluorescent PECAM1 Staining. Representative image of immunofluorescent PECAM1 staining used for vascular density analysis. PECAM1-stained endothelial cells can be easily seen lining vessels in the magnified section (yellow box). Image of 2-week tumor (NC) vasculature. (large image bar = 500 µM; magnified image bar = 250 µM).

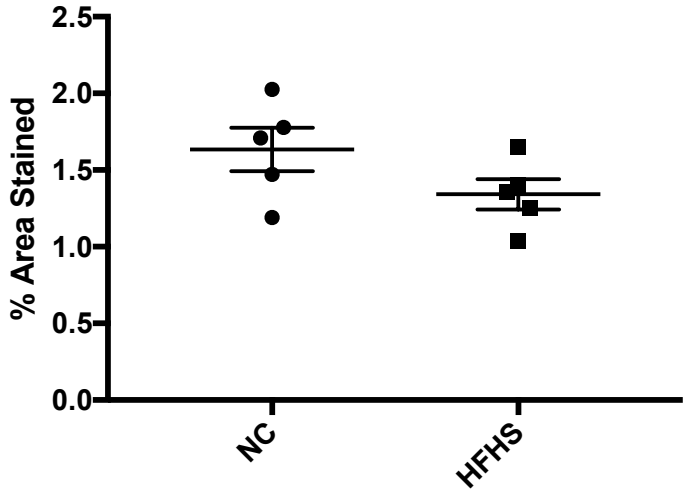

Figure 8: % Area of PECAM1 Staining (NC vs. HFHS). HFHS group shows slightly lower density of PECAM1 staining ($p = 0.1291$).

Some Vascularity Markers Showed a Lower Trend of Expression in Tumors from Diabetic Mice.

Western blots performed on the tumor samples showed different results depending on the time-course and the cohort of mice. 1-week tumors ($n = 4$, each) showed the following expression of proteins (**Figure 9A**). Of interest, the expressions of ACTA2 (NC vs. HFHS; 1 ± 0.1328 vs. 0.495 ± 0.103, $p = 0.0239$) and KDR (NC vs. HFHS; 1 ± 0.1463 vs. 0.4069 ± 0.05604, $p = 0.0091$) were significantly lower in the HFHS group compared to the control group (**Figure 9**).

GLRX (NC vs. HFHS; 1 ± 0.1536 vs. 0.4158 ± 0.009057, $p = 0.0090$) expression was also lower in the HFHS group (**Figure 9**). GLRX expression is decreased in ischemic muscles and skeletal muscle cells (unpublished data). The lower GLRX expression may indicate a hypoxic condition in tumors of the HFHS group.

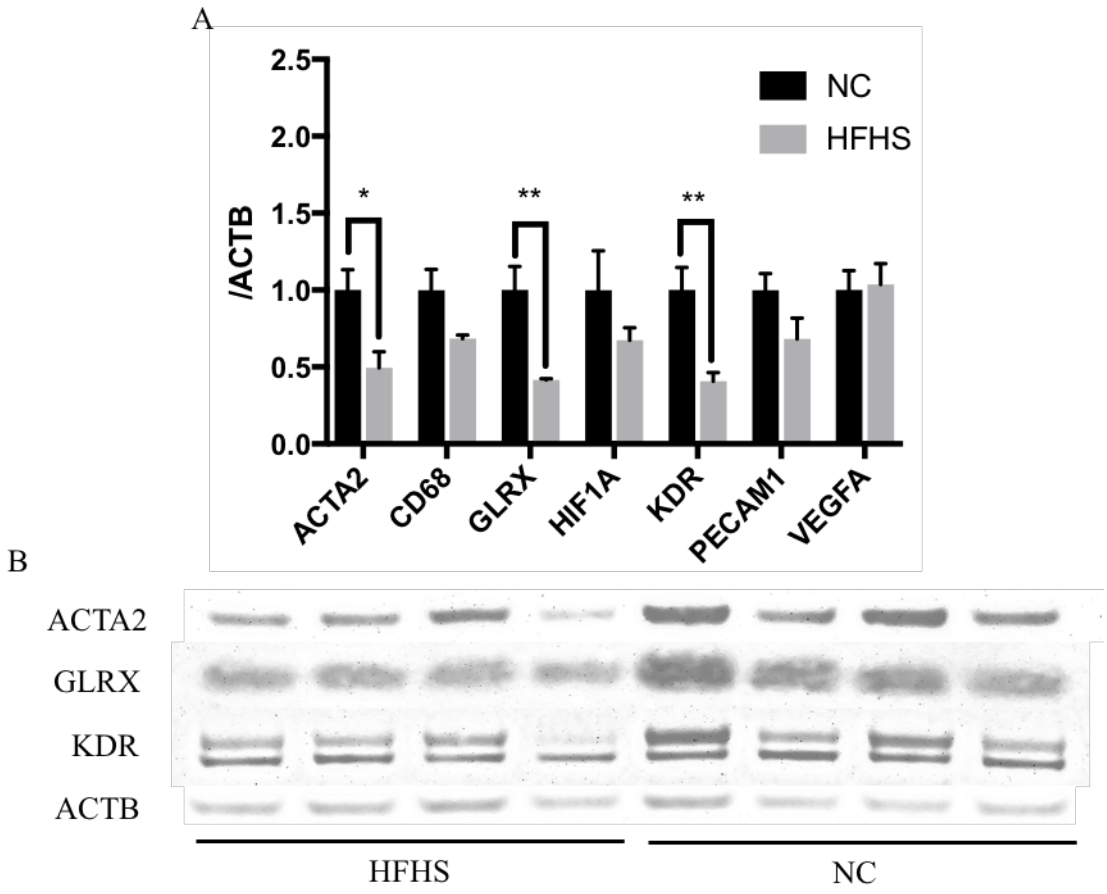

Figure 9: 1-Week Tumor Western Blot Protein Expression. (A) Summary of western blot results from 1-week tumor samples. Details of individual protein expression can be seen in the appendix. (* = $p \leq 0.05$; ** = $p \leq 0.01$). (B) Western blot of 1-week tumor proteins that show significant difference ($n = 4$, each).

The 2-week tumors excised from cohort 3 showed a similar expression of proteins with the following expressions (**Figure 10A**). All 3 proteins that were significantly different in the 1-week tumor retained their lower trend in the HFHS group. Although GLRX and KDR lost their significant difference, ACTA2 continued to retain a significant difference (NC vs. HFHS; 1 ± 0.04624 vs. 0.5586 ± 0.1215, $p = 0.0123$) (**Figure 10**).

These data indicate lower EC markers (ACTA2, KDR) in tumors from the HFHS-fed mice.

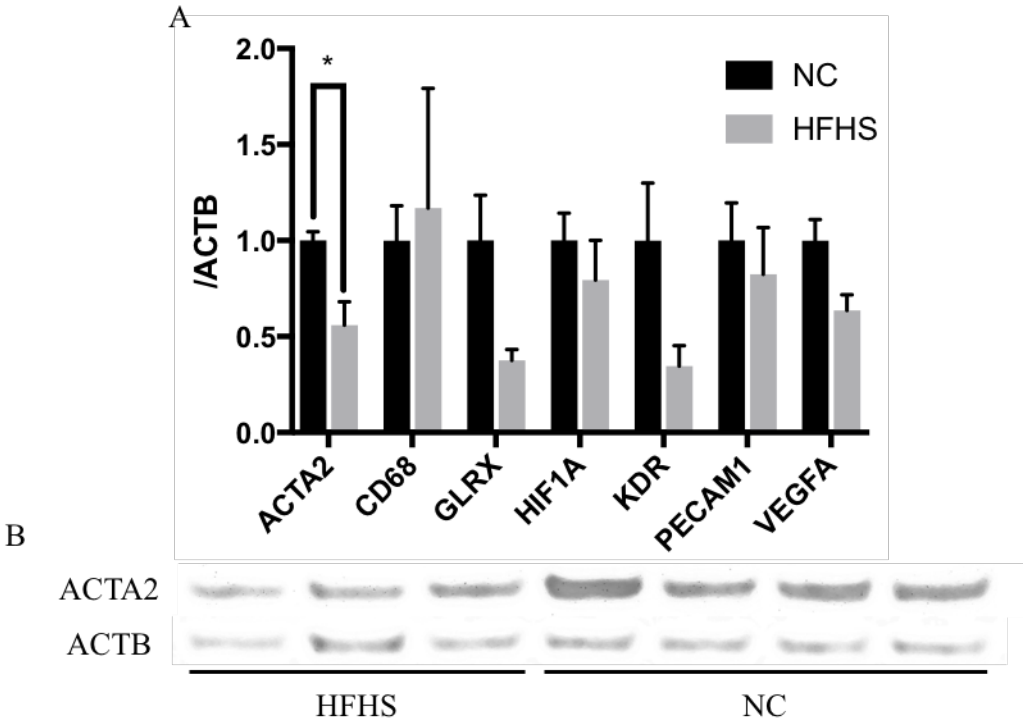

Figure 10: 2-Week Tumor (Cohort 3) Western Blot Protein Expression. (A) Summary of western blot results from 2-week tumor samples extracted from third cohort of mice. Details of individual protein expression can be seen in the appendix. (* = $p \leq 0.05$). (B) Western blot of ACTA2 from 2-week tumor samples (Cohort 3; $n = 3$, HFHS; $n = 4$, NC).

The 2-week tumors of the second cohort ($n = 5$, each) showed non-significant differences in the same angiogenic markers and proteins (**Table 3**, **Appendix**). Due to the inconsistency of results, the lower expression of vascular markers in diabetic tumors

cannot be concluded; however, it is worth reiterating that the vascularity of the tumor samples of the HFHS group were not increased despite the promoted tumor growth.

Interestingly, 2-week tumor samples from the HFHS group tended to show lower amounts of glutathionylated proteins compared to the NC group (**Figure 11**; Cohort 2, $p = 0.0317$), despite the lower trend in expressed GLRX. 1-week tumor samples ($n = 4$, each) of the HFHS group showed a slightly lower (1 ± 0.1156 vs. 0.9505 ± 0.1214), but not significant difference in glutathionylated proteins ($p = 0.7776$).

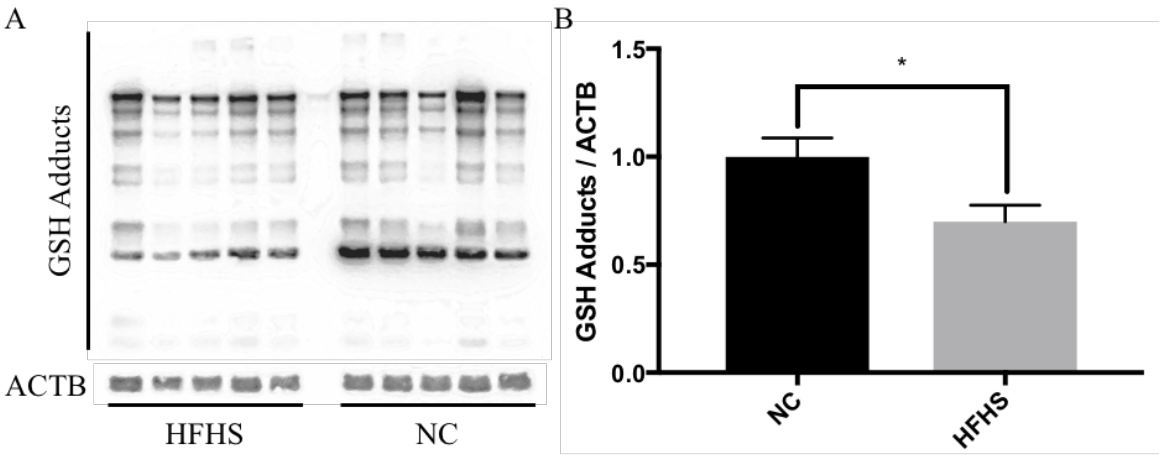

Figure 11: 2-Week Tumor GSH Adducts (Cohort 2). (A) Western blot of GSH adducts from 2-week tumor samples (Cohort 2; $n = 5$, each). (B) Summary of 2-week tumor (Cohort 2; $n = 5$, each) western blot of GSH adducts ($p = 0.0317$). (* = $p \leq 0.05$).

RT-qPCR analyses were performed on the 2-week tumor cohorts to examine the mRNA expression of angiogenic genes (PECAM1, VEGF, MMP2) and GLRX (**Figure 12**). No significant difference between NC and HFHS groups were observed.

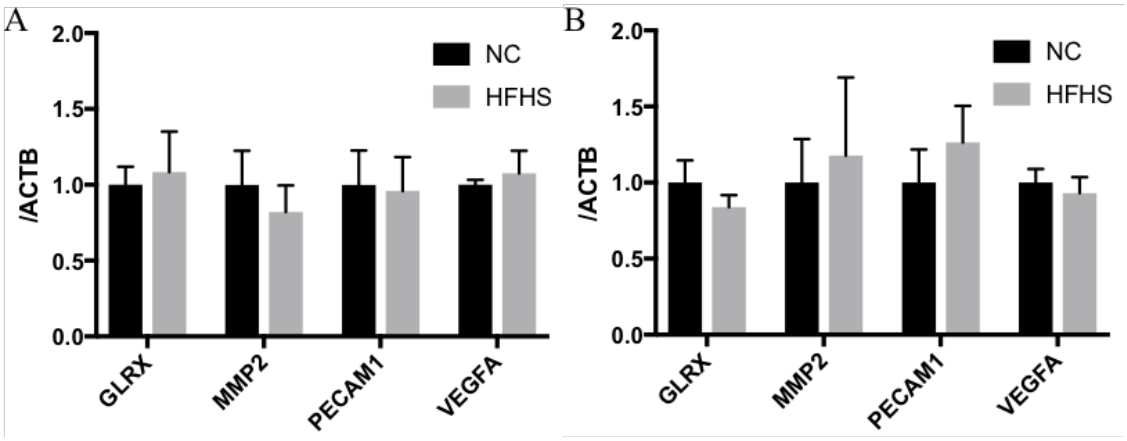

Figure 12: 2-Week Tumor RT-qPCR Results. (A) Summary of RT-qPCR results from tumor samples extracted from second cohort (n = 5, each). (B) Summary of RT-qPCR results from tumor samples extracted from third cohort (n = 4, NC; n = 3, HFHS). No significant difference was observed. Individual RT-qPCR results can be seen in the appendix.

High Glucose Inhibits Endothelial Cell Function *In Vitro*.

In order to determine the effects of hyperglycemia (4.5 g/L) on endothelial cells, cell-based assays were performed to assess its effect on proliferation, migration, and tube-forming capabilities, using normal medium as a low-glucose control (1.0 g/L). The results, however, need to be verified to make a definitive conclusion.

Cell proliferation assay results showed that high glucose impairs endothelial cell proliferation (**Figure 13**; p = 0.1548; n = 7, each).

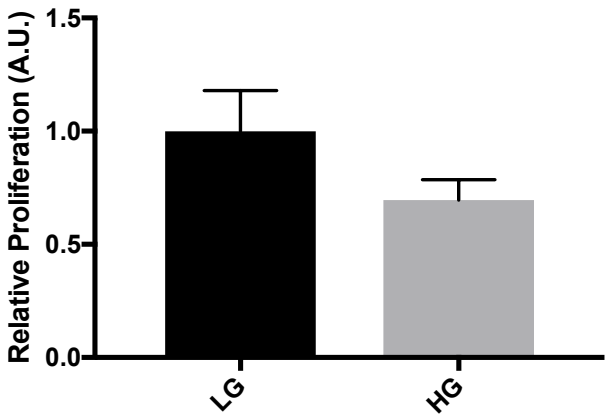

Figure 13: Endothelial Cell Proliferation Assay. High glucose inhibited endothelial cell proliferation ($p = 0.1548$; $n = 7$, each).

High glucose also attenuated endothelial cell migration in wound healing assays (**Figure 14**) performed both with ($p = 0.3388$) and without ($p = 0.4071$) VEGF for stimulation ($n = 3$, each).

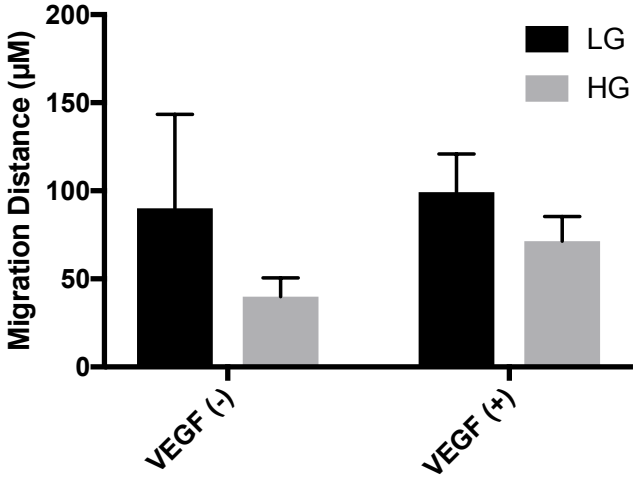

Figure 14: Endothelial Cell Wound Healing Assay. High glucose conditions inhibited endothelial cell migration both with ($p = 0.3388$) and without ($p = 0.4071$) VEGF stimulation ($n = 3$, each).

Matrigel-based tube-formation assays showed the ability of endothelial cells to form tubes was also repressed (**Figure 16**). The tube formation assays were skeletonized and quantified for the number of nodes, junctions, meshes, segments, and branches. The length of the segments and branches were also quantified alongside the total length (sum of the length of segments, isolated elements, and branches) and the areas of the meshes (**Figure 15**).

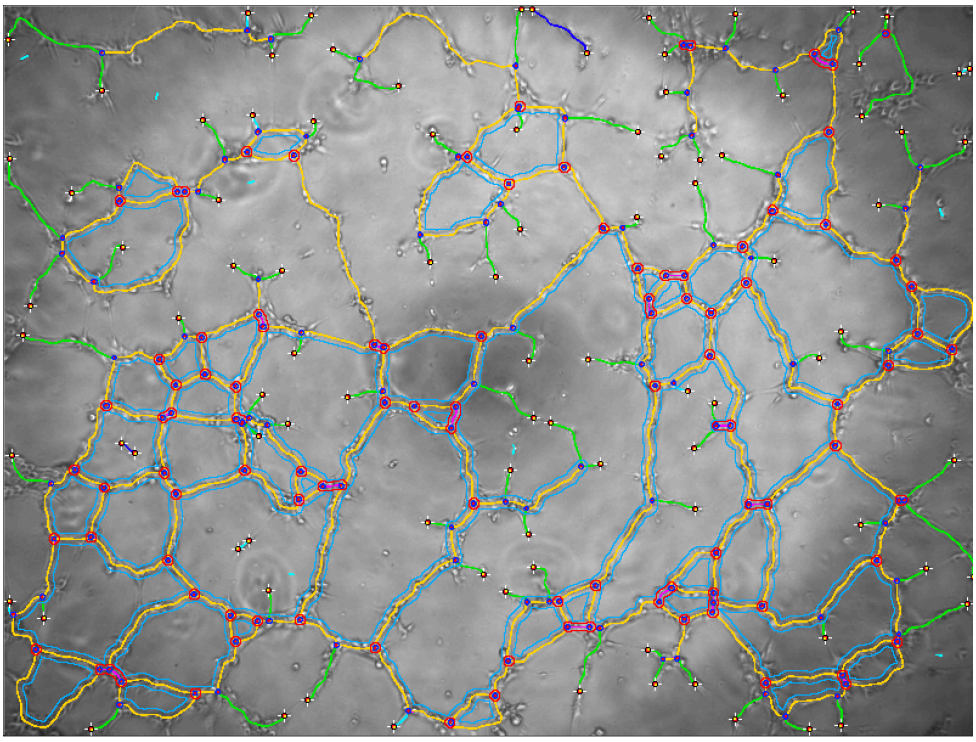

Figure 15: Angiogenesis Assay Analysis. Elements of the angiogenesis assay. (Elements used for analysis are highlighted in **bold**. **Green = Branches**; Cyan = Twigs; **Magenta = Segments**; Orange = Master Segments; **Sky Blue = Meshes**; **Red Surrounded by Blue = Nodes Surrounded by Junctions Symbol**; Junctions Surrounded by Red = Master Junctions; **Blue = Isolated Elements**; Cyan = Small Isolated Elements; Red Surrounded by Yellow = Extremities).

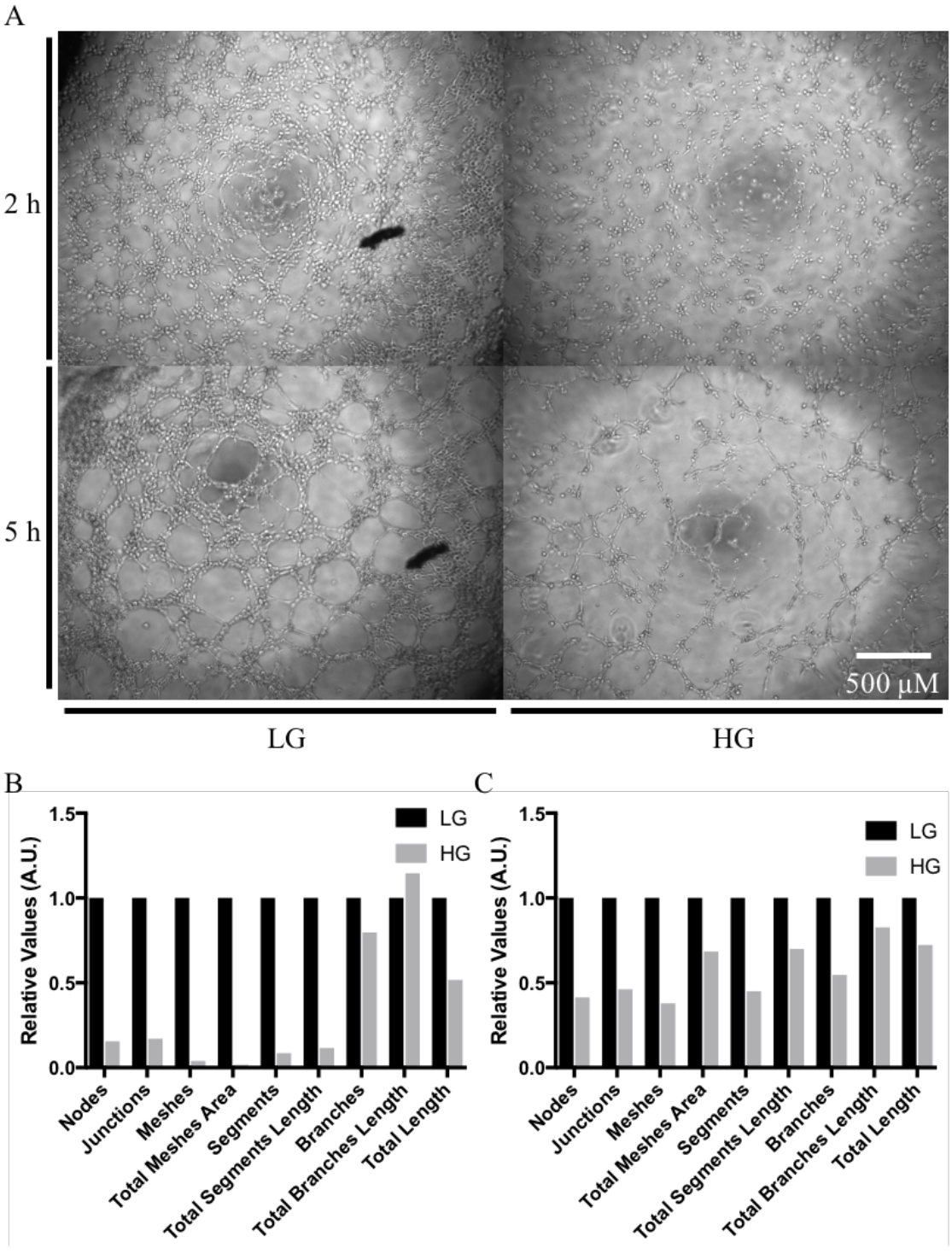

Figure 16: Matrigel-based EC Angiogenesis Assay. (A) Image of angiogenesis assay at 2 and 5 hours (LG vs. HG). (B) Qualitative measurements of angiogenesis assay (2h, *n* = 1, each). (C) Qualitative measurements of angiogenesis assay (5h, *n* = 1, each).

Also, interestingly, high glucose medium was able to promote a 1.45-fold increase of GLRX expression in endothelial cells (**Figure 17**; $n = 1$, each). This data, too, should be replicated for confidence.

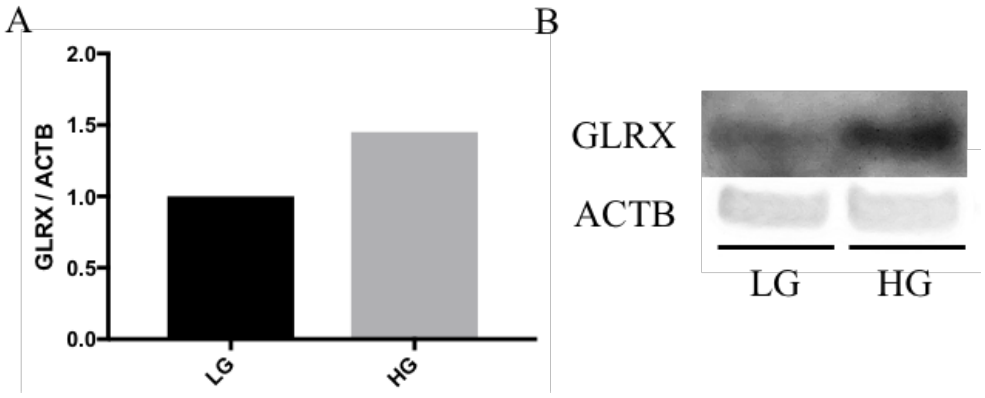

Figure 17: Effect of High Glucose on EC GLRX Expression. (A) High glucose promoted 1.45-fold increase in GLRX expression. (B) Western blot of EC GLRX expression (LG vs. HG).

In summary, the results of the study showed that T2DM induced by a HFHS diet is able to promote tumor growth in both weight (2-week, $p = 0.0070$) and volume (1-week, $p = 0.0351$; 2-week, $p = 0.0002$). Tumors extracted from the HFHS diet group showed reduced expressions of angiogenic markers (ACTA2 (1-week, $p = 0.0239$; 2-week, $p = 0.0123$), KDR (1-week, $p = 0.0091$)) by western blot and a slightly reduced trend of angiogenesis (PECAM1) in histological analyses. GLRX expression was reduced in HFHS tumor samples (1-week, $p = 0.0090$) and, interestingly, lower amounts of GSH adducts (2-week, $p = 0.0317$) could be seen in 2-week tumors as well. *In vitro* studies of endothelial cells show reduced trends of endothelial cell function (proliferation,

migration, and tube formation) in high glucose medium. Also, it has been observed that high glucose may be able to stimulate GLRX expression in endothelial cells.

DISCUSSION

The results of the following study have confirmed that B16F0 melanoma growth is, in fact, augmented in diet-induced diabetic mice; however, the vascular density and the expression of angiogenic markers from the tumor tissues did not parallel the growth in its size. *In vitro* studies suggested that high glucose can impair EC function (i.e. proliferation, migration, and tube formation capabilities) as well as promote GLRX expression, which may be related to this discrepancy. The mechanism of tumor growth in diabetes still lies inconclusive.

The Role of Angiogenesis in Diabetic Tumor Progression.

Despite the significantly enhanced tumor progression, which could be observed through the difference in 2-week tumor weights (NC vs. HFHS; 678.5 ± 43.54 mg, $n = 8$ vs. 1150 ± 147.6 mg, $n = 7$; $p = 0.007$), similar or slightly diminished trends in angiogenesis were observed in the tumor samples of the HFHS group (NC vs. HFHS; 1.635 ± 0.1418 % vs. 1.342 ± 0.09972 %; $p = 0.1291$; $n = 5$, each), and results of the western blot showed that certain angiogenic markers, KDR (1-week, $p = 0.0091$) and ACTA2 (2-week, $p = 0.0123$), were also significantly lower in the tumor samples of the HFHS mice. Although the results may coincide with the clinical manifestation of diabetes that show reduced angiogenesis in certain types of tissues (Kolluru, Bir, & Kevil, 2012), the results are of a puzzling nature as they seemingly undermine the notion that tumor growth should be angiogenesis-dependent (Nishida et al., 2006; Ronca et al., 2017).

The lower vascular density of the diabetic tumor samples may be the result of the impaired EC function (Zhu et al., 2015) and EC-GLRX expression observed in the hyperglycemia experiments *in vitro*. GLRX has been shown to be upregulated in diabetic rat tissue *in vivo* alongside high glucose experiments *in vitro* (Shelton et al., 2007). As GLRX is an NF-κB dependent gene (Aesif et al., 2011), the hyperglycemic environment alongside the inflammation associated with DM may have stimulated a higher level of GLRX to be expressed by endothelial cells *in vivo*, which could have decreased their migration capabilities (Cohen et al., 2016; Murdoch et al., 2014; Watanabe et al., 2016).

Thrombospondin-1 (THBS1) is another protein of interest that is shown to be implicated in the development of diabetic conditions and inhibited with hyperglycemia (Bhattacharyya et al., 2012). THBS1 is a potent endogenous inhibitor of angiogenesis (Bhattacharyya et al., 2012) and has been shown to be decreased in cancers where angiogenesis is increased (Stenina-Adognravi, 2014). miR-467, a tissue-specific transcriptional suppressor of THBS1, has been shown to be upregulated in hyperglycemic conditions *in vivo*, and also in tissues that are associated with increased angiogenesis in diabetic patients (Bhattacharyya et al., 2012; Krukovets et al., 2015). It is plausible that the non-significant difference between the angiogenesis of the two groups may be related to the close interplay between proangiogenic (e.g. miR-467) and antiangiogenic factors (e.g. GLRX).

EC-GLRX Expression May Be Related to Similar Vascular Density and Augmented Tumor Growth.

Another model in which augmented tumor growth can be seen without increased vascular density is a model of EC-specific GLRX-overexpressing transgenic mice (Matsui et al., 2017). Still under investigation, EC-specific GLRX-overexpressing transgenic mice were similarly implanted with subcutaneous B16F0 melanoma cells to test the hypothesis that decreased endothelial cell migration due to GLRX overexpression might hinder the growth of tumors. Interestingly enough, the mice of the transgenic study have shown to paradoxically exhibit an increased tumor growth, much like the diabetic mouse model, despite significantly decreased angiogenesis upon histological analysis of PECAM1 staining ($n = 6$, WT; $n = 5$, EC-GLRX TG; $p < 0.05$) (**Figure 18)**.

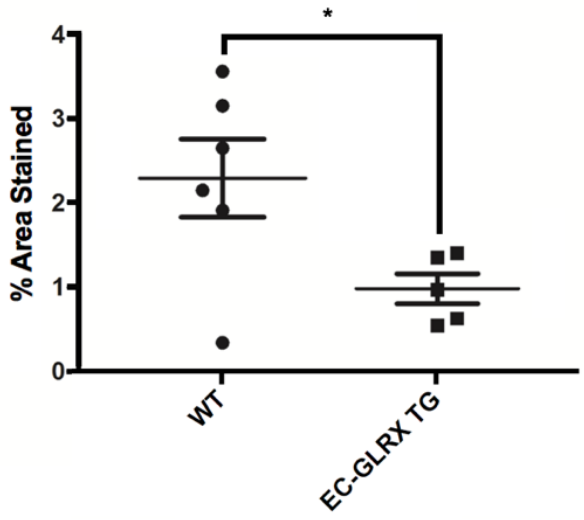

Figure 18: % Area of PECAM1 Staining (WT vs. EC-GLRX TG). Tumor samples extracted from EC-GLRX TG mice ($n = 5$) show a significantly lower density of PECAM1 staining compared to the wild-type (WT) ($n = 6$). (* = $p < 0.05$).

The *in vitro* high glucose experiments of the current study shows that it may be plausible that endothelial cells might be expressing higher levels of GLRX with diabetes *in vivo*, resulting in a similar outcome as those observed in the transgenic mice.

Tumor Cells May Be Displaying Vasculogenic Mimicry (VM) to Compensate for Impaired Angiogenesis.

If the above is true, and endothelial cells are, indeed, overexpressing GLRX in a diabetic system, the multiplex symptoms of diabetes can become more easily narrowed down to a single factor, i.e. hindered angiogenesis. Vascoulogenic mimicry is a concept in which certain malignant tumor cells have to potential to form vessel-like structures *de novo* and even differentiate into having EC-like capabilities if the blood supply is not sufficient (Delgado-Bellido et al., 2017; Qiao et al., 2015). Although the initial morphological, clinical, and molecular characterization of VM was carried out using human melanoma cells as a model, VM has also been observed in various malignant tumors, including glioblastoma, osteosarcoma, gallbladder, ovarian, lung, hepatocellular, breast, prostate, and gastric cancer, to name a few (Delgado-Bellido et al., 2017; Qiao et al., 2015).

If vasculogenic mimicry is present in the current study, it is plausible that tumor cells of the HFHS group may be expressing VM to compensate for the reduced blood supply and angiogenesis. The VM, that may not otherwise be as promoted in the control group, may be contributing to the augmented tumor growth in the diabetic model.

There are several methods to identify VM vessels, including PECAM1 - / PAS +, Dextran + / PECAM1 -, or even simple H & E staining of vessel-like structures without an EC-lined lumen (Delgado-Bellido et al., 2017; Qiao et al., 2015); however, the assessment of the qualitative characteristics of such structures still lie obscure as VM is a fairly newly discovered phenomenon. Interesting to note, however, is that WNT family member 5A (WNT5A) is known as one of the inducers for VM (Delgado-Bellido et al., 2017). WNT5A has previously been shown to be upregulated with diabetes (Aesif et al., 2011; Shelton et al., 2007) and GLRX overexpression through a positive feedback of the GLRX- NF-κB-WNT5A pathway (Murdoch et al., 2014). The corollary to these studies suggest that VM may be taking place in tumor samples of the T2DM mouse model. Further studies are required to elucidate this occurrence.

Other Possible Explanations for Enhanced Tumor Growth.

Type II diabetes mellitus, in likewise to cancer, is a complex multifactorial disorder that displays an array of different concomitant symptoms (Vigneri et al., 2009). Specifically, alongside hyperglycemia, obesity, inflammation, and insulin resistance are few of the many concurring symptoms of diabetes (American Diabetes Association, 2010; Centers for Disease Control and Prevention, 2017). In fact, cancer and T2DM share many of the same risk factors in the pathogeneses of the two diseases, such as aging, obesity, diet, and physical inactivity (Giovannucci et al., 2010). Because of such nature, the association between cancer and T2DM is that of a complex intertwined relationship. Possible mechanisms for the augmentation of cancer growth in T2DM include, but are

not limited to, hyperinsulinemia, hyperglycemia, inflammation, and adipokine secretion disturbances (Tahergorabi & Khazaei, 2012). Differences in diet may also lead to nutrient discrepancies, whereby tumor cells may be able to receive a more efficient and/or enriched nutrition to support its progression, which may also play a role in the augmentation of tumor sizes despite similar angiogenesis.

Limitations and Future Directions.

As stated above, since diabetes, specifically T2DM, is a complicated multifactorial condition. The following study has its limitations in aiming to focus on hyperglycemia, which represents just one of the multiple conjoining aspects and clinical manifestations of diabetes.

Cell-based assays were performed using HDMVEC instead of murine endothelial cells. If ECs were isolated from tumors, the diabetic EC from the tumor samples could have been characterized in detail (e.g. EC population, gene expression). Fluorescence activated cell sorting (FACS) methods have been attempted to isolate endothelial cells from the tumor samples (van Beijnum, Rousch, Castermans, van der Linden, & Griffioen, 2008); however, the population of endothelial cells in the tumor samples (approximately 1.5% of total mass by immunohistochemistry) posed a difficulty in the isolation, as the cell count was even lower after sorting. More specific markers and efficient methods for FACS isolation techniques need to be studied.

Future directions of this study should be aimed towards the explanation of the enhanced tumor growth in T2DM mice despite the similar vascular densities which were

observed to the control. Studies on the tumor samples should focus on markers pointed out through the discussion such as TBSP1 and WNT5A. Cadherin 5 (CDH5) may also be of significant interest, as the protein has been indicated to exhibit a particular functional significance in the VM of highly aggressive melanoma cells (Hendrix et al., 2001). *In vitro* endothelial cell studies should focus on the isolation of murine endothelial cells from tumor samples and verifying the effects of hyperglycemia on endothelial cell function and GLRX expression. The possibility of vasculogenic mimicry cannot be overlooked and histological analyses alongside FACS analyses could be the basis to understanding the presence of such phenomenon.

APPENDIX

Table 1. Tumor Measurements.

ID			*Tumor Measurements*					
Cohort & Diet		***Mouse Number***	***Incubation Period***	***Weight (mg)***	***L (mm)***	***W (mm)***	***H (mm)***	***V (mm^3)***
1 (Pilot)	*NC*	602-R	2 Weeks	3013.0	22.51	24.7	13.2	3842.8
		602-L	2 Weeks	1365.0	14.5	18.9	7.3	1047.5
		606-R	2 Weeks	519.0	13.47	8.84	6.89	429.6
		606-L	2 Weeks	2482.0	15.5	17.1	11.5	1596.0
		610-R	2 Weeks	2060.0	19.33	19.33	9.3	1819.5
	HFHS	618-R	2 Weeks	2468.0	22.02	17.45	11.95	2404.2
		618-L	2 Weeks	1261.0	15	10.52	7.84	647.8
		626-R	2 Weeks	444.0	12.14	10.92	6.68	463.7
		622-R	2 Weeks	996.0	18.24	11.27	11.5	1237.6
		622-L	2 Weeks	799.0	12.2	29.72	6.07	1152.4
2	*NC*	610-L	2 Weeks	615.0	17.3	6.8	5.6	344.9
		614-R	2 Weeks	818.0	19.4	10.8	5.9	647.3
		614-L	2 Weeks	572.0	8.0	16.4	5.5	377.8
		590-R	2 Weeks	499.0	20.4	7.4	3.7	292.5
		590-L	2 Weeks	633.0	10.4	14.2	7.9	610.9
	HFHS	630-R	2 Weeks	1421.0	24.8	14.4	10.2	1907.3
		630-L	2 Weeks	1296.0	22.7	14.6	8.5	1475.0
		594-R	2 Weeks	1003.0	18.5	13.9	9.4	1265.6
		594-L	2 Weeks	646.0	16.3	12.2	8.5	887.0
		626-L	2 Weeks	621.0	14.1	12.2	8.6	774.6
3	*NC*	983N	2 Weeks	860.0	10.4	7.3	15.2	604.2
		984R	2 Weeks	689.5	17.3	10.4	8.1	763.1
		985R	2 Weeks	741.6	8.3	5.9	18.5	474.4
		985N	2 Weeks	2516.0 *	15.6	21.4	12.3	2150.0 *
	HFHS	976R	2 Weeks	1594.1	14.3	20.8	11.6	1806.6
		976N	2 Weeks	1471.0	16.0	18.1	8.7	1319.2
		977R	2 Weeks	2985.0 *	30.1	18.1	11.4	3252.0 *
		977N **	2 Weeks	N/A	N/A	N/A	N/A	N/A

Table 1. Tumor Measurements (Continued).

ID			Tumor Measurements					
Cohort & Diet		***Mouse Number***	***Incubation Period***	***Weight (mg)***	***L (mm)***	***W (mm)***	***H (mm)***	***V (mm^3)***
4	*NC*	984N	1 Week	83.1	4.4	4.5	2.2	22.8
		986R	1 Week	107.8	7.9	5.4	1.9	42.4
		986N	1 Week	66.5	7.5	4.2	1.6	26.4
		987N	1 Week	136.4	6.3	4.8	3.4	53.8
	HFHS	978N	1 Week	119.0	7.6	9.3	3.1	114.7
		979R	1 Week	158.4	4.9	17.2	3.5	154.5
		979N	1 Week	140.5	7.6	10.1	2.2	88.4
		829N	1 Week	111.8	8.0	8.5	1.3	46.3

* = Significant outliers ($p < 0.05$) were omitted in the analyses of results.
** = Mouse was found dead 1-week post-implantation.

Table 2. Protein Expression in 1-Week Tumor Samples.

Protein of Interest	***NC (n = 4)***	***HFHS (n = 4)***	***p***
*ACTA2 **	1 ± 0.1328	0.495 ± 0.103	0.0239
CD68	1 ± 0.1352	0.6834 ± 0.02389	0.0607
*GLRX ***	1 ± 0.1536	0.4158 ± 0.009057	0.009
HIF1A	1 ± 0.2547	0.6745 ± 0.08145	0.2691
*KDR ***	1 ± 0.1463	0.4069 ± 0.05604	0.0091
PECAM1	1 ± 0.1083	0.6824 ± 0.1351	0.1163
VEGFA	1 ± 0.1265	1.036 ± 0.1371	0.8549
GSH Adducts	1 ± 0.1156	0.9505 ± 0.1214	0.7776

* = $p \leq 0.05$, ** = $p \leq 0.01$.

Table 3. Protein Expression in 2-Week Tumor Samples (Cohort 2).

Protein of Interest	*NC (n = 5)*	*HFHS (n = 5)*	*p*
ACTA2	1 ± 0.3044	0.8683 ± 0.1555	0.7101
CD68	1 ± 0.1536	1.192 ± 0.1999	0.4692
GLRX	1 ± 0.1748	1.491 ± 0.2755	0.1711
HIF1A	1 ± 0.1447	1.056 ± 0.2827	0.8649
KDR	1 ± 0.1239	1.046 ± 0.1508	0.8188
PECAM1	1 ± 0.1486	1.555 ± 0.2492	0.0919
VEGFA	1 ± 0.09522	0.9024 ± 0.08169	0.4591
GSH Adducts *	1 ± 0.0864	0.6992 ± 0.07698	0.0317

* = $p \leq 0.05$.

Table 4. Protein Expression in 2-Week Tumor Samples (Cohort 3).

Protein of Interest	*NC (n = 4)*	*HFHS (n = 3)*	*p*
*ACTA2**	1 ± 0.04624	0.5586 ± 0.1215	0.0123
CD68	1 ± 0.1803	1.168 ± 0.6235	0.7771
GLRX	1 ± 0.2364	0.3754 ± 0.0573	0.079
HIF1A	1 ± 0.1431	0.7946 ± 0.2065	0.4346
KDR	1 ± 0.2987	0.3465 ± 0.1064	0.1329
PECAM1	1 ± 0.1961	0.8245 ± 0.2439	0.5945
VEGFA	1 ± 0.1094	0.6364 ± 0.08081	0.0552
GSH Adducts	1 ± 0.1297	0.9243 ± 0.2243	0.7675

* = $p \leq 0.05$.

Table 5. 2-Week Tumor RT-qPCR Results (Pilot Cohort).

Protein of Interest	*NC (n = 5)*	*HFHS (n = 5)*	*p*
ANGPT2	1 ± 0.1603	1.618 ± 0.4319	0.2169
FLT1	1 ± 0.124	1.171 ± 0.2537	0.5623
GLRX	1 ± 0.1581	0.9491 ± 0.1799	0.8371
HIF1A	1 ± 0.05256	0.9255 ± 0.03067	0.2557
MMP2 *	1 ± 0.3359	2.499 ± 0.4472	0.0279
PECAM1 *	1 ± 0.1874	1.817 ± 0.2834	0.0429
TXN	1 ± 0.07965	0.8442 ± 0.07344	0.1882
VEGFA	1 ± 0.1465	1.032 ± 0.1266	0.872

Results of the pilot cohort may not be reliable as results from the latter cohorts. Tumors exhibited severe skeletal muscle and skin invasion at the time of extraction.
* = $p \leq 0.05$.

Table 6. 2-Week Tumor RT-qPCR Results (Cohort 2).

Protein of Interest	*NC (n = 5)*	*HFHS (n = 5)*	*p*
GLRX	1 ± 0.03231	1.076 ± 0.1492	0.6341
MMP2	1 ± 0.1184	1.084 ± 0.2676	0.7825
PECAM1	1 ± 0.2262	0.9596 ± 0.2222	0.9017
VEGFA	1 ± 0.2243	0.8201 ± 0.1764	0.5459

Table 7. 2-Week Tumor RT-qPCR Results (Cohort 3).

Protein of Interest	*NC (n = 4)*	*HFHS (n = 3)*	*p*
GLRX	1 ± 0.08909	0.9303 ± 0.1059	0.6341
MMP2	1 ± 0.1464	0.8384 ± 0.07897	0.4233
PECAM1	1 ± 0.2168	1.264 ± 0.241	0.4551
VEGFA	1 ± 0.2857	1.178 ± 0.5125	0.7581

REFERENCES

Aesif, S. W., Kuipers, I., van der Velden, J., Tully, J. E., Guala, A. S., Anathy, V., . . . Janssen-Heininger, Y. M. (2011). Activation of the glutaredoxin-1 gene by nuclear factor kappaB enhances signaling. *Free Radical Biology and Medicine, 51*(6), 1249-1257. doi:10.1016/j.freeradbiomed.2011.06.025

American Diabetes Association. (2010). Diagnosis and Classification of Diabetes Mellitus. *Diabetes Care, 33*(Suppl 1), S62-S69. doi:10.2337/dc10-S062

Ayala, J. E., Samuel, V. T., Morton, G. J., Obici, S., Croniger, C. M., Shulman, G. I., . . . McGuinness, O. P. (2010). Standard operating procedures for describing and performing metabolic tests of glucose homeostasis in mice. *Disease Models & Mechanisms, 3*(9-10), 525-534. doi:10.1242/dmm.006239

Barone, B. B., Yeh, H. C., Snyder, C. F., Peairs, K. S., Stein, K. B., Derr, R. L., . . . Brancati, F. L. (2008). Long-term all-cause mortality in cancer patients with preexisting diabetes mellitus: a systematic review and meta-analysis. *JAMA, 300*(23), 2754-2764. doi:10.1001/jama.2008.824

Barone, B. B., Yeh, H. C., Snyder, C. F., Peairs, K. S., Stein, K. B., Derr, R. L., . . . Brancati, F. L. (2010). Postoperative mortality in cancer patients with preexisting diabetes: systematic review and meta-analysis. *Diabetes Care, 33*(4), 931-939. doi:10.2337/dc09-1721

Bhattacharyya, S., Sul, K., Krukovets, I., Nestor, C., Li, J., & Adognravi, O. S. (2012). Novel Tissue‐Specific Mechanism of Regulation of Angiogenesis and Cancer Growth in Response to Hyperglycemia. *Journal of the American Heart Association: Cardiovascular and Cerebrovascular Disease, 1*(6), e005967. doi:10.1161/JAHA.112.005967

Centers for Disease Control and Prevention. (2017). National Diabetes Statistics Report, 2017. *Atlanta, Ga: Centers for Disease Control and Prevention, U.S. Dept of Health and Human Services*.

Chen, S. C., Su, Y. C., Lu, Y. T., Ko, P. C., Chang, P. Y., Lin, H. J., . . . Lai, Y. P. (2014). Defects in the acquisition of tumor-killing capability of CD8+ cytotoxic T cells in streptozotocin-induced diabetic mice. *PloS One, 9*(11), e109961. doi:10.1371/journal.pone.0109961

Cheng, R., & Ma, J. X. (2015). Angiogenesis in diabetes and obesity. *Reviews in Endocrine & Metabolic Disorders, 16*(1), 67-75. doi:10.1007/s11154-015-9310-7

Cohen, R. A., Murdoch, C. E., Watanabe, Y., Bolotina, V. M., Evangelista, A. M., Haeussler, D. J., . . . Matsui, R. (2016). Endothelial Cell Redox Regulation of Ischemic Angiogenesis. *Journal of Cardiovascular Pharmacology, 67*(6), 458-464. doi:10.1097/fjc.0000000000000381

Delgado-Bellido, D., Serrano-Saenz, S., Fernandez-Cortes, M., & Oliver, F. J. (2017). Vasculogenic mimicry signaling revisited: focus on non-vascular VE-cadherin. *Molecular Cancer, 16*(1), 65. doi:10.1186/s12943-017-0631-x

Duh, E. J., Sun, J. K., & Stitt, A. W. (2017). Diabetic retinopathy: current understanding, mechanisms, and treatment strategies. *JCI Insight, 2*(14), e93751. doi:10.1172/jci.insight.93751

Giovannucci, E., Harlan, D. M., Archer, M. C., Bergenstal, R. M., Gapstur, S. M., Habel, L. A., . . . Yee, D. (2010). Diabetes and cancer: a consensus report. *Diabetes Care, 33*(7), 1674-1685. doi:10.2337/dc10-0666

Hendrix, M. J., Seftor, E. A., Meltzer, P. S., Gardner, L. M., Hess, A. R., Kirschmann, D. A., . . . Seftor, R. E. (2001). Expression and functional significance of VE-cadherin in aggressive human melanoma cells: role in vasculogenic mimicry. *Proceedings of the National Academy of Sciences of the United States of America, 98*(14), 8018-8023. doi:10.1073/pnas.131209798

Kolluru, G. K., Bir, S. C., & Kevil, C. G. (2012). Endothelial Dysfunction and Diabetes: Effects on Angiogenesis, Vascular Remodeling, and Wound Healing. *International Journal of Vascular Medicine, 2012*, 918267. doi:10.1155/2012/918267

Krukovets, I., Legerski, M., Sul, P., & Stenina-Adognravi, O. (2015). Inhibition of hyperglycemia-induced angiogenesis and breast cancer tumor growth by systemic injection of microRNA-467 antagonist. *FASEB Journal, 29*(9), 3726-3736. doi:10.1096/fj.14-267799

Matsui, R., Watanabe, Y., & Murdoch, C. E. (2017). Redox regulation of ischemic limb neovascularization - What we have learned from animal studies. *Redox Biol, 12*, 1011-1019. doi:10.1016/j.redox.2017.04.040

Mori, A., Sakurai, H., Choo, M. K., Obi, R., Koizumi, K., Yoshida, C., . . . Saiki, I. (2006). Severe pulmonary metastasis in obese and diabetic mice. *International Journal of Cancer, 119*(12), 2760-2767. doi:10.1002/ijc.22248

Murdoch, C. E., Shuler, M., Haeussler, D. J., Kikuchi, R., Bearelly, P., Han, J., . . . Matsui, R. (2014). Glutaredoxin-1 up-regulation induces soluble vascular endothelial growth factor receptor 1, attenuating post-ischemia limb revascularization. *Journal of Biological Chemistry, 289*(12), 8633-8644. doi:10.1074/jbc.M113.517219

Nishida, N., Yano, H., Nishida, T., Kamura, T., & Kojiro, M. (2006). Angiogenesis in Cancer. *Vascular Health and Risk Management, 2*(3), 213-219.

Novosyadlyy, R., Lann, D. E., Vijayakumar, A., Rowzee, A., Lazzarino, D. A., Fierz, Y., . . . LeRoith, D. (2010). Insulin-mediated acceleration of breast cancer development and progression in a nonobese model of type 2 diabetes. *Cancer Research, 70*(2), 741-751. doi:10.1158/0008-5472.CAN-09-2141

Nunez, N. P., Oh, W. J., Rozenberg, J., Perella, C., Anver, M., Barrett, J. C., . . . Vinson, C. (2006). Accelerated tumor formation in a fatless mouse with type 2 diabetes and inflammation. *Cancer Research, 66*(10), 5469-5476. doi:10.1158/0008-5472.CAN-05-4102

Qiao, L., Liang, N., Zhang, J., Xie, J., Liu, F., Xu, D., . . . Tian, Y. (2015). Advanced research on vasculogenic mimicry in cancer. *Journal of Cellular and Molecular Medicine, 19*(2), 315-326. doi:10.1111/jcmm.12496

Racordon, D., Valdivia, A., Mingo, G., Erices, R., Aravena, R., Santoro, F., . . . Owen, G. I. (2017). Structural and functional identification of vasculogenic mimicry in vitro. *Scientific Reports, 7*(1), 6985. doi:10.1038/s41598-017-07622-w

Ronca, R., Benkheil, M., Mitola, S., Struyf, S., & Liekens, S. (2017). Tumor angiogenesis revisited: Regulators and clinical implications. *Medicinal Research Reviews, 37*(6), 1231-1274. doi:10.1002/med.21452

Shelton, M. D., Kern, T. S., & Mieyal, J. J. (2007). Glutaredoxin regulates nuclear factor kappa-B and intercellular adhesion molecule in Muller cells: model of diabetic retinopathy. *Journal of Biological Chemistry, 282*(17), 12467-12474. doi:10.1074/jbc.M610863200

Spreen, M. I., Gremmels, H., Teraa, M., Sprengers, R. W., Verhaar, M. C., Statius van Eps, R. G., . . . van Overhagen, H. (2016). Diabetes Is Associated With Decreased Limb Survival in Patients With Critical Limb Ischemia: Pooled Data From Two Randomized Controlled Trials. *Diabetes Care, 39*(11), 2058-2064. doi:10.2337/dc16-0850

Stenina-Adognravi, O. (2014). Invoking the power of thrombospondins: Regulation of thrombospondins expression. *Matrix Biology, 37*, 69-82. doi:https://doi.org/10.1016/j.matbio.2014.02.001

Tahergorabi, Z., & Khazaei, M. (2012). Imbalance of Angiogenesis in Diabetic Complications: The Mechanisms. *International Journal of Preventive Medicine, 3*(12), 827-838.

Tomayko, M. M., & Reynolds, C. P. (1989). Determination of subcutaneous tumor size in athymic (nude) mice. *Cancer Chemotherapy and Pharmacology, 24*(3), 148-154.

van Beijnum, J. R., Rousch, M., Castermans, K., van der Linden, E., & Griffioen, A. W. (2008). Isolation of endothelial cells from fresh tissues. *Nature Protocols, 3*(6), 1085-1091. doi:10.1038/nprot.2008.71

Varu, V. N., Hogg, M. E., & Kibbe, M. R. (2010). Critical limb ischemia. *Journal of Vascular Surgery, 51*(1), 230-241. doi:10.1016/j.jvs.2009.08.073

Vigneri, P., Frasca, F., Sciacca, L., Pandini, G., & Vigneri, R. (2009). Diabetes and cancer. *Endocrine-Related Cancer, 16*(4), 1103-1123. doi:10.1677/erc-09-0087

Watanabe, Y., Murdoch, C. E., Sano, S., Ido, Y., Bachschmid, M. M., Cohen, R. A., & Matsui, R. (2016). Glutathione adducts induced by ischemia and deletion of glutaredoxin-1 stabilize HIF-1alpha and improve limb revascularization. *Proceedings of the National Academy of Sciences of the United States of America, 113*(21), 6011-6016. doi:10.1073/pnas.1524198113

Zhu, Z. X., Cai, W. H., Wang, T., Ye, H. B., Zhu, Y. T., Chi, L. S., . . . Jin, L. T. (2015). bFGF-Regulating MAPKs Are Involved in High Glucose-Mediated ROS Production and Delay of Vascular Endothelial Cell Migration. *PloS One, 10*(12), e0144495. doi:10.1371/journal.pone.0144495

CURRICULUM VITAE